Available online at www.sciencedirect.com

ScienceDirect

IFAC PapersOnline CONFERENCE PAPER ARCHIVE

IFAC PapersOnLine 55-1 (2022) 492–497

Acceleration control-aided APDG law for powered descent landing in atmospheric conditions

Kedarisetty Siddhardha * **Joel George Manathara** **

* *Postdoctoral Fellow, Department of Aerospace Engineering, Indian Institute of Science, Bengaluru-560012, India (e-mail: siddhardhak2010@gmail.com)*

** *Assistant Professor, Department of Aerospace Engineering, Indian Institute of Technology Madras, Chennai-600036, India*

Abstract

Apollo powered descent guidance (APDG) law enabled Apollo lunar module to land on the Moon successfully. Since then, in the past 50 years, APDG and several of its variants have been used in numerous planetary landing studies and missions. As its formulation does not consider drag force, the APDG law is typically used for powered descent landing in rarefied environments like the Moon and Mars. In this paper, we extend the application of the APDG law to atmospheric environments by aiding it with an acceleration controller. The proposed acceleration control strategy not only compensates for the estimated aerodynamic drag, but also mitigates the uncertainties in the thrust produced, thus maintaining the desired acceleration. To demonstrate the efficacy, we provide results of simulated powered descent landing of a reusable launch vehicle (RLV) on Earth using the proposed acceleration control strategy along with the APDG law.

Keywords: Acceleration control, atmospheric flight, powered descent landing, Apollo powered descent guidance, reusable launch vehicles

1. INTRODUCTION

Stepping foot on the Moon was one of the greatest achievements of humankind. The dream of going to the Moon became a reality owing to the conglomeration of advanced technologies and novel ideas during that period. One such technological innovation, which even to date continues to find applications, is the Apollo-powered descent guidance (APDG) technology (Klumpp, 1974).

Over 50 years ago, APDG law was used to land the Apollo lunar module on the Moon. This guidance law commands the desired thrust for a lander to reach a specified final position and velocity at a specified time based on its current position and time. APDG law is considered elegant not only due to its ability to make the vehicle reach its target satisfying the specified constraints, but also due to its simplicity and ease of implementation. As a result, APDG scheme has become the baseline descent guidance for various planetary missions.

Following the invention of the APDG law, there appeared several variations of it such as tunable APDG, universal powered guidance, and augmented APDG (Lu, 2018; Lu et al., 2018; Lu, 2019). Nevertheless, the structure of all these guidance laws is the same as that of the APDG law.

Apart from the closed-form guidance laws such as APDG and its variants, many optimal guidance methods have also been developed for powered descent landing. Most of the works–be it APDG variants or optimal guidance techniques–provide guidance solutions for landing on the Moon or Mars, but not on Earth. Therefore, in developing these guidance laws, the influence of aerodynamic drag is neglected owing to the rarefied atmosphere in which the vehicles employing these guidance laws are expected to operate.

The atmospheric influence near to Earth's surface is, however, not negligible. Only a handful of works are available on powered descent landing on Earth. The challenges involved in powered descent and landing in the presence of aerodynamic drag and the recent advances on the precision landing of reusable rockets on Earth have been summarized in Blackmore (2016). Szmuk et al. (2016) posed powered landing in aerodynamic environments as a second-order cone programming problem and found fuel-optimal optimal trajectories via successive convex programming approach. Wenzel et al. (2018) improved the numerical conditioning of the second-order cone programming problem for fuel-optimal trajectories in atmospheric conditions using different transcription methods such as pseudospectral and multiple shooting to make the real-time optimal guidance implementation possible. Ma et al. (2018) presented a direct trajectory optimization framework for powered descent and landing of reusable rockets with restartable engines in atmospheric environments. That work was further extended to multi-point guidance for planetary soft landings (Ma et al., 2019). Wang et al. (2020) solved the fuel-optimal Earth-landing problem of reusable rockets in two parts. First, considering the drag to be zero, they performed a lossless convexification of

10.1016/j.ifacol.2022.04.081

the problem and solved it, and in the later iterations, homotopically added the drag profile to the problem.

Although it is possible to obtain fuel-optimal solutions for powered descent in atmospheric conditions from numerical optimal guidance techniques, APDG variants are at times still preferred. This is because the fuel-optimal trajectories are not much different from the trajectory solutions provided by the APDG variants, and for this reason, the solutions from the APDG laws act as baseline for evaluating the performances of the numerical optimal guidance schemes. Further, owing to their closed-form solutions, the APDG variants are computationally light, and therefore, on-board and real-time friendly.

Unlike in the numerical optimal guidance formulations where drag is a part of the Earth descent and landing problem, APDG does not consider atmospheric drag in its formulation. As a result, when APDG is used on a vehicle in atmospheric conditions, the vehicle will not follow the desired accelerations commanded by the APDG law. Nevertheless, the final velocity and position constraints will be satisfied owing to the feedback nature of APDG.

To demonstrate the ability of APDG to satisfy the final position and velocity constraints in spite of drag, a powered landing simulation is performed for a reusable launch vehicle (RLV) using the APDG law in Earth's environment. The simulation assumes RLV to be a rigid body with its trajectory restricted to the vertical plane (x-z plane). The simulation is performed with initial position and velocity of the RLV as (0 m, 10000 m) and (200 ms^{-1}, $-500\,\mathrm{ms}^{-1}$), and the desired final position and velocity as (8000 m, 0 m) and (0 ms^{-1}, $-1\,\mathrm{ms}^{-1}$). The time for flight is specified as 50 seconds. The results of this simulation are presented in Figure 1. From this figure, we can observe that the accelerations of RLV (a_x, a_z) do not follow the desired accelerations (a_{x_d}, a_{z_d}) specified by the APDG law except towards the end of the specified time at which point the speed of the vehicle is very low for the drag to be validly neglected, and yet it reaches the target position with the desired velocity.

In many planetary landing scenarios, APDG ensures that the RLV satisfy the final velocity and position constraints regardless the presence of the atmosphere (Strohl III, 2018). Nevertheless, there exist a few scenarios where the desired accelerations must be satisfied throughout the flight. For example, consider that the landing zone has obstacles due to uneven mountainous terrain. In such a case, the accelerations provided by the guidance law that ensure collision-free trajectory must be closely followed. This requires an acceleration control law to compensate for the drag unaccounted by the guidance law.

Acceleration controllers are often used as inner loop controllers of the translation control subsystem to enhance trajectory tracking capabilities (Alkowatly et al., 2015; Alexis et al., 2012). However, these controllers reduce the acceleration errors but do not drive them to zero. Afman et al. (2018) used a triple integral controller to maintain desired acceleration of multirotor unmanned aerial vehicles (UAVs) in the presence of aerodynamic drag at low airspeeds. In our previous works, we designed an acceleration control law for multirotor UAVs to maintain the desired acceleration despite the atmospheric disturbances and performed vertical maneuvers to enable reduced gravity environments (Kedarisetty and Manathara, 2019; Kedarisetty, 2019; Siddhardha, 2019).

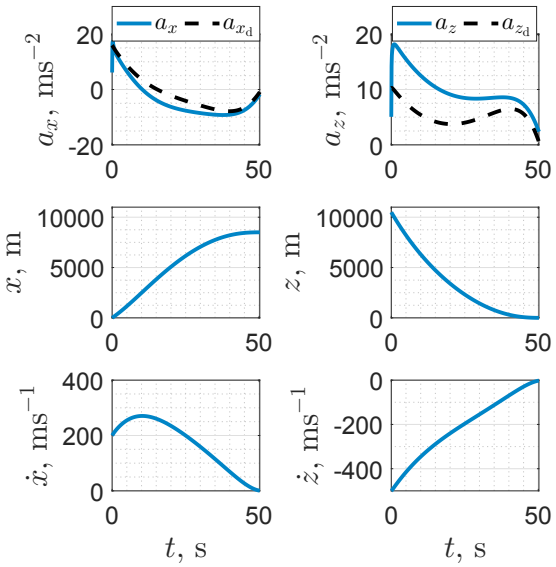

Figure 1. APDG law based powered descent of RLV in Earth's environment

This paper presents an acceleration control technique that will follow the desired acceleration commands provided by the APDG law even in atmospheric environments. The advantage of this control technique is that it can compensate for uncertainties in drag as well as thrust due to atmospheric presence and/or engine performance. The efficacy of the suggested acceleration control law was demonstrated in (Kedarisetty and Manathara, 2019) for one dimensional (vertical) acceleration control for multirotor unmanned aerial vehicles at low airspeeds. In the current paper, we show that this control law can be used for the RLV landing problem where very high velocities are involved. Further, we demonstrate that the application of this control law can be extended to lateral dimensions with a few modifications. The efficacy of the APDG law augmented with the proposed acceleration control law is established through simulations.

2. APOLLO POWERED DESCENT GUIDANCE

This section discusses preliminaries on APDG law. The APDG law requires a specified time for the mission, and therefore, the method to estimate the final time to land is also discussed. As stated earlier, in deriving APDG law, drag is neglected. The powered descent vehicle (an RLV, for the purpose of this paper) is considered to be a point mass with descent dynamics as

$$\begin{aligned} \dot{\boldsymbol{r}} &= \boldsymbol{V} \\ \boldsymbol{a} = \dot{\boldsymbol{V}} &= \boldsymbol{g} + \frac{\boldsymbol{T}}{m} \end{aligned} \tag{1}$$

where m is the mass of the RLV, $\boldsymbol{r} = [x,\, z]^{\mathrm{T}}$ is its position, $\boldsymbol{V} = [\dot{x},\, \dot{z}]^{\mathrm{T}}$ is the velocity, $\boldsymbol{a} = [\ddot{x},\, \ddot{z}]^{\mathrm{T}}$ is the acceleration, $\boldsymbol{T} = [T_x,\, T_z]^{\mathrm{T}}$ is the thrust generated by the RLV, and $\boldsymbol{g}$ is the acceleration due to gravity. Note that all the above quantities are expressed in the Earth frame.

The APDG law commands the desired acceleration vector ($\boldsymbol{a}_\mathrm{d}$) at time t as (Klumpp, 1974)

$$\boldsymbol{a}_\mathrm{d} = -\frac{6}{t_\mathrm{go}}\left[\boldsymbol{V}_\mathrm{f} - \boldsymbol{V}\right] + \frac{12}{t_\mathrm{go}^2}\left[\boldsymbol{r}_\mathrm{f} - \boldsymbol{r} - \boldsymbol{V}t_\mathrm{go}\right] + \boldsymbol{a}_\mathrm{f} \tag{2}$$

where t_f is the specified final time, $t_\mathrm{go} = t_\mathrm{f} - t$, and $\boldsymbol{r}_\mathrm{f}$ and $\boldsymbol{V}_\mathrm{f}$ are the prescribed position and velocity vectors, respectively, at the specified final time.

A reasonable estimate of t_f, which is required for the APDG law, can be obtained by solving the following polynomial (D'Souza and D'Souza, 1997)

$$t_\mathrm{f}^4 + k_2 t_\mathrm{f}^2 + k_1 t_\mathrm{f} + k_0 = 0 \tag{3}$$

where $k_2 = -2\boldsymbol{V}_\mathrm{i}\cdot\boldsymbol{V}_\mathrm{i}/\Lambda$, $k_1 = -12\boldsymbol{V}_\mathrm{i}\cdot\boldsymbol{r}_\mathrm{i}/\Lambda$, and $k_0 = -18\boldsymbol{r}_\mathrm{i}\cdot\boldsymbol{r}_\mathrm{i}/\Lambda$. Here the subscript 'i' represents the initial condition, and $\Lambda = \Gamma + \boldsymbol{g}\cdot\boldsymbol{g}/2$. Γ is a weighting parameter on the final time – a larger Γ yields a lower time to land. The value of Γ used for the simulations presented in this paper is 20000.

By generating the thrust $\boldsymbol{T} = m\boldsymbol{a}_\mathrm{d}$, an RLV in the absence of atmosphere follows the desired acceleration. However, as shown in Figure 1, by generating thrust equal to mass times the desired acceleration is not sufficient to converge the RLV's acceleration to the desired value in the presence of an atmosphere, in which case the total acceleration is the sum of the accelerations due to thrust and drag. Towards faithfully following the desired acceleration in spite of the presence of drag which was not accounted for in the formulation of the guidance law, a model-based acceleration control law is suggested. The model used for this purpose is presented in the following section.

3. MATHEMATICAL MODEL

In this section, the mathematical model of RLV under the assumption that its motion is restricted to the vertical plane (x-z plane) with z-axis in the vertical direction is presented. The governing equations of the RLV model are

$$\begin{aligned} \dot{\boldsymbol{r}} &= \boldsymbol{V} \\ m\dot{\boldsymbol{V}} &= \boldsymbol{T} + \boldsymbol{D} + m\boldsymbol{g} \\ \dot{m} &= -\alpha\left\|\boldsymbol{T}\right\|_2 \\ \ddot{\theta} &= -2\zeta\omega\dot{\theta} - \omega^2\theta + \omega^2\theta_\mathrm{d} \end{aligned} \tag{4}$$

where θ is the RLV's pitch angle. The thrust generated by RLV in the Earth reference frame $\boldsymbol{T} = [T_x,\, T_z]^\mathrm{T}$ can be expressed in terms of θ as $[T\sin\theta,\, T\cos\theta]^\mathrm{T}$, where T is the total thrust generated by the RLV. The drag is expressed as $\boldsymbol{D} = -\frac{1}{2}\rho S C_D \left\|\boldsymbol{V}\right\|\boldsymbol{V}$, where C_D is the drag coefficient, S is the reference area, and ρ is the ambient density which is evaluated as $\rho = 1.225e^{-0.000096z}$. The mass dissipation rate constant (due to fuel consumption) is expressed as $\alpha = \dfrac{1}{I_\mathrm{sp} g_0}$, where I_sp is the specific impulse and g_0 is the acceleration due to Earth's gravity at sea level. The vehicle's pitch angle is assumed to follow a second-order dynamics with ζ and ω as the damping constant and natural frequency of the dynamics. The vehicle parameters are provided in Table 1.

The thrust generated by the RLV for a given desired thrust (T_d) is modeled as the following first-order dynamical system

Table 1. RLV parameters

m_0 (kg)	m_dry (kg)	I_sp (s)	S (m^2)	C_D	ζ	ω (Hz)
35000	25000	400	10.75	0.5	1.2	5

$$\dot{T} = -\frac{1}{\tau}\left(T - T_\mathrm{loss}\right) + \frac{1}{\tau}T_\mathrm{d} \tag{5}$$

where τ (taken as 0.05 s for the simulations) is the thrust time constant. The thrust loss (T_loss) due to wake dispersion in the presence of atmosphere is given as (Haidn, 2008)

$$T_\mathrm{loss} = PA, \quad P = 101325e^{-0.00012z}\,\mathrm{Nm}^{-2} \tag{6}$$

where P is the free stream pressure and A is the engine throat area which is chosen to be 1.2 m^2.

The thrust dynamics, incorporating the uncertainties, can also be written as

$$\dot{T} = -\frac{1}{\tau}T + \frac{k_T}{\tau}T_\mathrm{d} \tag{7}$$

where k_T is the thrust gain. Thrust time constant incorporates the delay within the engine to generate the desired thrust, and steady-state thrust gain incorporates the thrust losses that occur due to wake dispersion in atmosphere and engine performance uncertainties. As described in the next section, the proposed acceleration controller makes use of k_T to compensate for atmospheric drag and the uncertainties in the thrust produced by the engine.

4. ACCELERATION CONTROLLER

In this section, a model-based acceleration controller to maintain the desired acceleration despite the drag force and engine uncertainties is designed. Towards this, first, the mathematical model of RLV presented in the previous section is simplified by assuming that the thrust dynamics are negligible ($\tau \approx 0$). The simplified RLV acceleration model, written as components along x and z axes, is

$$\begin{aligned} ma_x &= k_x T_{x_\mathrm{d}} - k_D|\dot{x}|\dot{x} \\ ma_z &= k_z T_{z_\mathrm{d}} - k_D|\dot{z}|\dot{z} - mg \end{aligned} \tag{8}$$

where k_x and k_z are the steady state thrust gains in x and z directions, and $k_D = \dfrac{1}{2}\rho S C_D$ is the drag constant. From Equation (8), we can obtain the following control law–desired thrust–in order to maintain the desired accelerations a_{x_d} and a_{z_d}.

$$\begin{aligned} T_{x_\mathrm{d}} &= \frac{m}{\hat{k}_x}\left(a_{x_\mathrm{d}} + \frac{\hat{k}_D}{m}|\dot{x}|\dot{x}\right) \\ T_{z_\mathrm{d}} &= \frac{m}{\hat{k}_z}\left(a_{z_\mathrm{d}} + \frac{\hat{k}_D}{m}|\dot{z}|\dot{z} + g\right) \end{aligned} \tag{9}$$

In the above set of equations, '$\hat{}$' represents the estimate of the corresponding quantity.

The proposed control law in Equation (9) requires the estimates of the steady-state thrust gains and drag constant. However, accurately calculating the steady-state thrust gains and the drag coefficient individually requires experimental data and testing. Therefore, we give a method to estimate steady-state thrust gains from the axial velocity and acceleration measurements. The steady-state gains are estimated as follows.

$$\hat{k}_x = \frac{ma_x + \hat{k}_D|\dot{x}|\dot{x}}{T_{x_\mathrm{d}}}$$
$$\hat{k}_z = \frac{m\left(a_z + g\right) + \hat{k}_D|\dot{z}|\dot{z}}{T_{z_\mathrm{d}}} \tag{10}$$

For implementation, we use discrete forms of the proposed acceleration control and steady-state thrust gain estimation schemes, which, for the n^{th} time step, are given as:

$$T_{x_\mathrm{d}}[n] = \frac{m}{\hat{k}_x[n-1]}\left(a_{x_\mathrm{d}}[n] + \frac{\hat{k}_D}{m}|\dot{x}[n]|\dot{x}[n]\right)$$
$$T_{z_\mathrm{d}}[n] = \frac{m}{\hat{k}_z[n-1]}\left(a_{z_\mathrm{d}}[n] + \frac{\hat{k}_D}{m}|\dot{z}[n]|\dot{z}[n] + g\right)$$
$$\hat{k}_x[n] = \frac{ma_x[n] + \hat{k}_D|\dot{x}[n]|\dot{x}[n]}{T_{x_\mathrm{d}}[n]} \tag{11}$$
$$\hat{k}_z[n] = \frac{m\left(a_z[n] + g\right) + \hat{k}_D|\dot{z}[n]|\dot{z}[n]}{T_{z_\mathrm{d}}[n]}$$

Note that the above scheme requires $\hat{k}_D$ – the estimate of the drag constant. It can be shown that the performance of the proposed acceleration controller is invariant to the value of $\hat{k}_D$ used to a large extent (Kedarisetty and Manathara, 2019). Thus, choosing a reasonable estimate of k_D would suffice for the actual acceleration to closely follow the desired acceleration. To demonstrate this, in the simulations conducted in this paper, we use an estimate of the drag constant that is 40% higher than the actual value (that is, we use $\hat{k}_D = 1.4k_D$). The exact conditions on $\hat{k}_D$ under which the convergence of the proposed scheme is guaranteed when the vehicle motion is restricted to vertical direction is derived in Kedarisetty and Manathara (2019). A similar approach can be followed in the current situation where the vehicle is also allowed to move in a lateral direction.

A few more modifications for the developed acceleration control strategy are essential before its implementation. From Equation (11), we can observe that if the desired thrusts tend to zero, then steady-state thrust gain estimates tend to infinity. To prevent that, we use the following fix.

$$T_{x_\mathrm{d}} = 0.1\mathrm{sgn}(T_{x_\mathrm{d}}), \quad \text{if } |T_{x_\mathrm{d}}| \leq 0.1\,\mathrm{N}$$
$$\mathrm{sgn}(T_{x_\mathrm{d}}) = \begin{cases} 1, & \text{if } T_{x_\mathrm{d}} > 0 \\ 0, & \text{if } T_{x_\mathrm{d}} = 0 \\ -1, & \text{if } T_{x_\mathrm{d}} < 0 \end{cases} \tag{12}$$

The acceleration controller in Equation (11) is developed under the assumption that the thrust dynamics are negligible. Therefore, to take into account the thrust dynamics, that is, to ensure that the generated commands can be faithfully followed even in the presence of engine dynamics, we introduce a steady-state gain low-pass filter with a time constant (τ_k) greater than that of the thrust dynamics. The filtered steady-state thrust gains are given as

$$\hat{k}_x^\mathrm{f}[n] = \frac{\Delta t}{\Delta t + \tau_\mathrm{k}}\hat{k}_x[n] + \frac{\tau_\mathrm{k}}{\Delta t + \tau_\mathrm{k}}\hat{k}_x^\mathrm{f}[n-1]$$
$$\hat{k}_z^\mathrm{f}[n] = \frac{\Delta t}{\Delta t + \tau_\mathrm{k}}\hat{k}_z[n] + \frac{\tau_\mathrm{k}}{\Delta t + \tau_\mathrm{k}}\hat{k}_z^\mathrm{f}[n-1] \tag{13}$$

Table 2. Simulation parameters

Parameter	Value
$\boldsymbol{r}_\mathrm{i}$	$[0\,\mathrm{m},\ 10000\,\mathrm{m}]^\mathrm{T}$
$\boldsymbol{V}_\mathrm{i}$	$[200\,\mathrm{ms}^{-1},\ -500\,\mathrm{ms}^{-1}]^\mathrm{T}$
$\boldsymbol{r}_\mathrm{f}$	$[8000\,\mathrm{m},\ 0\,\mathrm{m}]^\mathrm{T}$
$\boldsymbol{V}_\mathrm{f}$	$[0\,\mathrm{ms}^{-1},\ -1\,\mathrm{ms}^{-1}]^\mathrm{T}$
θ_i	$50\,\mathrm{deg}$
$\dot{\theta}_\mathrm{i}$	$0\,\mathrm{deg\,s}^{-1}$
t_f	$50.72\,\mathrm{s}$

where Δt (taken as 0.01 s for simulations) is the sampling time and τ_k (taken as 1 s) is the low-pass filter time constant. These filtered steady-state thrust gains are used in calculating the desired thrust as

$$T_{x_\mathrm{d}}[n] = \frac{m}{\hat{k}_x^\mathrm{f}[n-1]}\left(a_{x_\mathrm{d}}[n] + \frac{\hat{k}_D}{m}|\dot{x}[n]|\dot{x}[n]\right)$$
$$T_{z_\mathrm{d}}[n] = \frac{m}{\hat{k}_z^\mathrm{f}[n-1]}\left(a_{z_\mathrm{d}}[n] + \frac{\hat{k}_D}{m}|\dot{z}[n]|\dot{z}[n] + g\right) \tag{14}$$

The developed acceleration control strategy is validated through simulations in the next section.

5. SIMULATION RESULTS

In this section, we present the results of two simulations of the powered descent landing of RLV on Earth. APDG with PID acceleration control law is used in the first simulation, and the APDG law with the proposed acceleration strategy is used in the second simulation. The initial and final conditions for both these simulations are presented in Table 2. The time of flight for these simulations is estimated to be 50 seconds using Equation (3) and the parameters provided in Table 2.

The results of the powered descent landing of RLV simulation using APDG law with PID acceleration control law are presented in Figure 2. From Figures 2a and 2b, we can observe that the final position and velocity constraints are satisfied. This is expected as even without any acceleration control the APDG law can satisfy the final position and velocity constraints as was shown in the simulation in Section 1 (refer Figure 1). As can be observed from Figures 2c and 1, the acceleration errors when the APDG law is aided with a PID acceleration controller is less compared to APDG law without any acceleration control. Nevertheless, acceleration errors still exist, especially during the initial part of descent along the vertical axis. During the initial part of the descent, the acceleration errors are high because of the high drag force due to high initial velocities. However, as the velocity reduced, the acceleration of RLV converged to the desired value.

In the second simulation, the drag coefficient is assumed to be 40% higher than the actual value ($\hat{k}_D = \frac{1}{2}\rho S \times 1.4C_D$), and the value of k_T which incorporates the thrust loss due to plume impingement is considered to be unknown.

The simulation results for RLV landing using APDG and the proposed control law are presented in Figure 3. From this figure, we can observe that the final position and velocity constraints are satisfied. Moreover, the RLV faithfully tracks the desired acceleration commanded by the

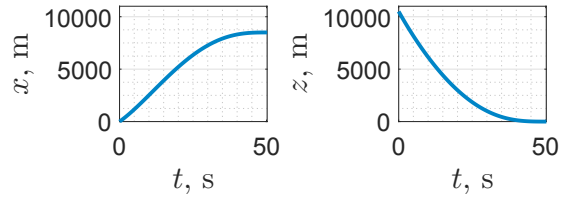

(a) Positions

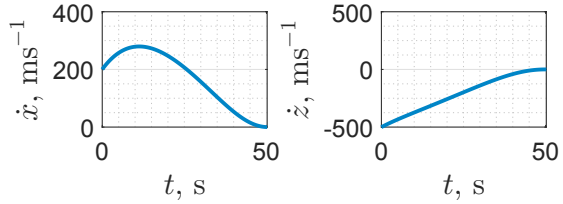

(b) Velocities

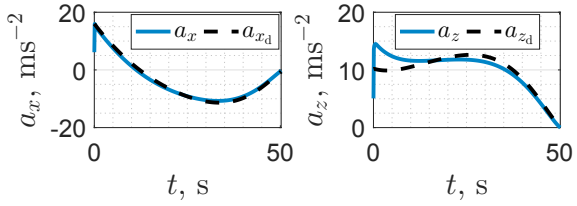

(c) Accelerations

Figure 2. RLV powered descent landing in Earth environment using the APDG law along with PID acceleration controller

APDG law throughout the descent despite drag uncertainties. This faithful acceleration tracking is attributed to the proposed acceleration control strategy. A momentary deviation from the desired acceleration in the x-axis at the 20-second mark can be observed in Figure 3c. This is due to the steady-state thrust gain estimate ($\hat{k}_x$) reaching its limiting value. $\hat{k}_x$ reaches its bounds due to the zero-crossing of the desired thrust along the x-axis, as seen in Figure 3e. Note that $\hat{k}_x$ and $\hat{k}_z$ estimators compensated for the drag coefficient estimation error along with the thrust loss due to plume impingement and maintained the RLV's acceleration at the desired value.

Table 3. Root mean square error of the RLV's acceleration

Acceleration controller	x-axis	z-axis
None	$4.9451\,\mathrm{ms}^{-2}$	$8.2819\,\mathrm{ms}^{-2}$
PID controller	$2.5407\,\mathrm{ms}^{-2}$	$4.0791\,\mathrm{ms}^{-2}$
Model-based controller	$2.0573\,\mathrm{ms}^{-2}$	$1.9148\,\mathrm{ms}^{-2}$

The root mean square deviation of the acceleration from the desired value obtained through simulating the powered descent landing of the RLV using APDG, PID acceleration controller aided APDG, and the model-based acceleration controller aided APDG are presented in Table 3. From this table, we can observe that the proposed model-based acceleration controller aided APDG performs better than the other two methods. With the proposed acceleration controller, the acceleration errors occur only during initial transients and while $\hat{k}_x$ reaches its bounds. Thus from comparative results presented in Table 3, we can conclude that the APDG law aided with the proposed acceleration

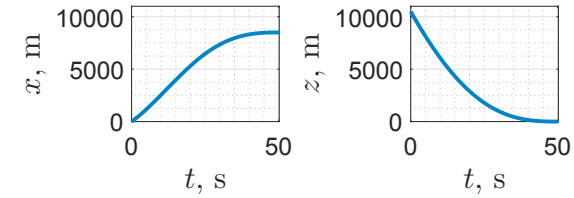

(a) Positions

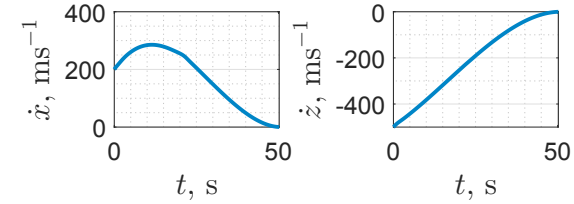

(b) Velocities

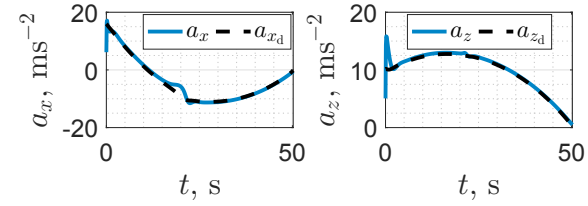

(c) Accelerations

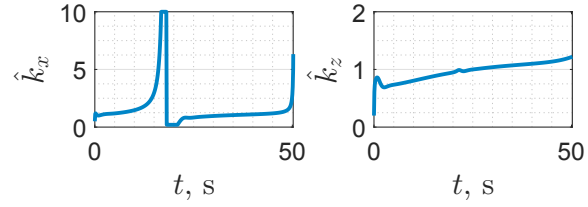

(d) Estimated thrust gains

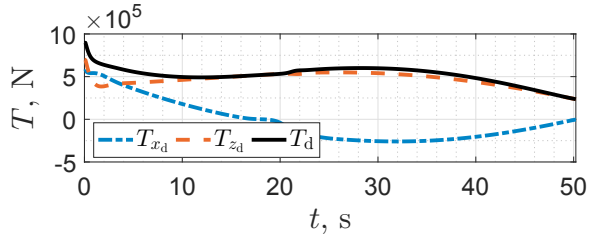

(e) Desired thrust

Figure 3. RLV powered descent landing in Earth environment using the APDG law along with the proposed acceleration controller

control strategy can be used to powered descent landing in atmospheric conditions while maintaining the desired accelerations.

6. CONCLUSION

In this paper, we showed that the APDG law could be extended to powered descent landing of RLV in atmospheric environments when aided with an acceleration controller. Towards this, we proposed a model-based acceleration control law that can maintain the desired acceleration by compensating for the drag force despite parameter uncertainties in the model. Simulations were performed to show the efficacy of the proposed control law. The proposed acceleration controller can be used in tandem with any

guidance law that commands a desired thrust and can be extended to other powered flight regimes of RLVs.

REFERENCES

Afman, J.P., Feron, E., and Hauser, J. (2018). Triple-integral control for reduced-g atmospheric flight. In *Proc. of 2018 Annual American Control Conference (ACC)*, 392–397. IEEE, Milwaukee, USA.

Alexis, K., Nikolakopoulos, G., and Tzes, A. (2012). Model predictive quadrotor control: attitude, altitude and position experimental studies. *IET Control Theory & Applications*, 6(12), 1812–1827.

Alkowatly, M.T., Becerra, V.M., and Holderbaum, W. (2015). Body-centric modelling, identification, and acceleration tracking control of a quadrotor UAV. *International journal of modelling, identification and control*, 24(1), 29–41.

Blackmore, L. (2016). Autonomous precision landing of space rockets. *Frontiers of Engineering: Reports on Leading-Edge Engineering*, 46, 15–20.

D'Souza, C. and D'Souza, C. (1997). An optimal guidance law for planetary landing. In *AIAA Guidance, Navigation, and Control Conference*, 1–6. Orleans, USA.

Haidn, O.J. (2008). Advanced rocket engines. *Advances on Propulsion Technology for High-speed Aircraft*, 1, 6.1–6.40.

Kedarisetty, S. (2019). Model based robust control and automation design for a micro-gravity enabling multi-rotor test bed. In *AIAA Guidance, Navigation, and Control Conference*, 1–11. San Diego, USA.

Kedarisetty, S. and Manathara, J.G. (2019). Acceleration control of a multi-rotor UAV towards achieving micro-gravity. *Aerospace Systems*, 2(2), 175–188.

Klumpp, A.R. (1974). Apollo lunar descent guidance. *Automatica*, 10(2), 133–146.

Lu, P. (2018). Propellant-optimal powered descent guidance. *Journal of Guidance, Control, and Dynamics*, 41(4), 813–826.

Lu, P. (2019). Augmented apollo powered descent guidance. *Journal of Guidance, Control, and Dynamics*, 42(3), 447–457.

Lu, P., Sostaric, R.R., and Mendeck, G.F. (2018). Adaptive powered descent initiation and fuel-optimal guidance for mars applications. In *2018 AIAA Guidance, Navigation, and Control Conference*, 0616. Kissimmee, USA.

Ma, L., Wang, K., Xu, Z., Shao, Z., and Song, Z. (2018). Trajectory optimization for powered descent and landing of reusable rockets with restartable engines. In *Proc. of International Astronautical Congress*. Bremen, Germany.

Ma, L., Wang, K., Xu, Z., Shao, Z., Song, Z., and Biegler, L.T. (2019). Multi-point powered descent guidance based on optimal sensitivity. *Aerospace Science and Technology*, 86, 465–477.

Siddhardha, K. (2019). Autonomous reduced-gravity enabling quadrotor test-bed: Design, modelling and flight test analysis. *Aerospace Science and Technology*, 86, 64–77.

Strohl III, L.D. (2018). *An Evaluation of Apollo Powered Descent Guidance*. Ph.D. thesis, San Diego State University.

Szmuk, M., Acikmese, B., and Berning, A.W. (2016). Successive convexification for fuel-optimal powered landing with aerodynamic drag and non-convex constraints. In *Proc. of AIAA Guidance, Navigation, and Control Conference*, 0378. San Diego, USA.

Wang, J., Li, H., and Chen, H. (2020). An iterative convex programming method for rocket landing trajectory optimization. *The Journal of the Astronautical Sciences*, 67(4), 1553–1574.

Wenzel, A., Sagliano, M., and Seelbinder, D. (2018). Performance analysis of real-time optimal guidance methods for vertical take-off, vertical landing vehicles. In *Proc. of International Astronautical Congress*. Bremen, Germany.